Carbohydrate Polymers 200 (2018) 321–331

Contents lists available at ScienceDirect

Carbohydrate Polymers

journal homepage: www.elsevier.com/locate/carbpol

Salicylic acid loaded chitosan microparticles applied to lettuce seedlings: Recycling shrimp fishing industry waste

Sergio Martin-Saldaña[a,*], Merari Tumin Chevalier[b,1], Maria José Iglesias[c,1], Silvana Lorena Colman[c,1], Claudia Anahí Casalongué[c], Vera Alejandra Álvarez[b], Alberto Antonio Chevalier[a]

[a] Gihon Laboratorios Químicos SRL, Mar del Plata, Argentina
[b] UNMdP, CONICET, Instituto de Investigación en Ciencia & Tecnología de Materiales INTEMA, Grupo Materiales Compuestos Termoplásticos CoMP, Mar Del Plata, Argentina
[c] Instituto de Investigaciones Biológicas, UE CONICET-UNMDP, Facultad de Ciencias Exactas y Naturales, Universidad Nacional de Mar del Plata, Mar del Plata, Argentina

ARTICLE INFO

Keywords:
Chitosan
Salicylic acid
Microparticles
Lettuce
Plant defense response

ABSTRACT

Shrimp fishing industry wastes are still a main problem with high environmental impact worldwide. In this study, chitosan with ultra-high molecular weight and deacetylation degree ≥85% was obtained from shrimp fishing industry waste from Argentinean Patagonia. Chitosan based microparticles capable to entrap salicylic acid, a phytohormone known to play major role in the regulation of plant defense response against various pathogens, were prepared using TPP as crosslinker. Unloaded microparticles and microparticles loading several salicylic acid amount were fully characterized exhibiting a size between 1.57 μm and 2.45 μm. Furthermore, a good PDI, entrappment efficiencies from 59% to 98% and salicylic acid sustained release over 24 h were achieved.

Chitosan based microparticles were non toxic in most of the doses applied in lettuce seedlings. Instead, microparticles can positively modulate plant growth and have the potential to improve plant defense responses. In particular salicylic acid loaded microparticles effect was very promising for its application as activators of salicylic acid dependent plant defense responses in lettuce as a model of horticultural plant species.

1. Introduction

Chitosan (CS) is the second most abundant polysaccharide in nature after cellulose, and it is a deacetylated derivative of chitin found mainly in the exoskeletons of crustaceans (Kanmani, Jeyaseelan, Kamaraj, Sureshbabu, & Sivashanmugam, 2017). CS is a polycationic heteropolysaccharide consisting of two monosaccharides, N-acetyl-glucosamine and D-glucosamine which relative amounts could varies in a wide range, yielding CS of varying degrees of deacetylation ranging from 75% to 95% (Tharanathan & Kittur, 2003). In addition, CS has functional groups which play an important role in its functionalities. The most important one is the amino group, specially in acidic conditions, which allows CS to interact with negatively charged molecules due to the protonation phenomenon (Bellich, D'Agostino, Semeraro, Gamini, & Cesàro, 2016).

Since CS could be produced from chitin obtained from fishing waste by exhaustive alkaline deacetylation, many commercial applications of CS and its derivatives have been explored (Bellich et al., 2016). This polymer combines several properties such as biocompatibility, biodegradability, nontoxicity and bioadhesion, which make it valuable compound for biomedical (Dash, Chiellini, Ottenbrite, & Chiellini, 2011), pharmaceutical (Yang et al., 2017), food (Atay et al., 2017; Prashanth & Tharanathan, 2007), waste water treatment (Kanmani et al., 2017), and agricultural applications (El Hadrami, Adam, El Hadrami, & Daayf, 2010) among others.

In agriculture, the use of toxic pesticides to control plant diseases is a common practice which cause hazards to the human health and environment (Mishra, Keswani, Abhilash, Fraceto, & Singh, 2017). Despite the valuable contribution of new pesticides to control plant diseases, smart and sustainable options to develop a bioplaguicide as an alternative to agro-chemicals still remains as a challenge in phytopathology. In this sense, CS has been proved as an environmental-friendly polymer for agricultural uses due to its wide spectrum biological activity including antimicrobial effect against many bacteria,

* Corresponding author.
E-mail address: martin.saldana@gihonlab.com (S. Martin-Saldaña).
[1] Authors contributed equally for this work.

https://doi.org/10.1016/j.carbpol.2018.08.019
Received 11 April 2018; Received in revised form 5 August 2018; Accepted 5 August 2018
Available online 06 August 2018

fungi and yeasts, with a lower toxicity toward mammalian cells (Kong, Chen, Xing, & Park, 2010) and induce host defense responses in both monocotyledons and dicotyledons (El Hadrami et al., 2010). CS is also considered to be an applicable elicitor by triggering host defense respones in both mono and dicotyledon plants (Ryan, 1987). Elicitors in plant biology are extrinsic or foreign molecules often associated with plant pests, diseases or synergistic organisms. The term plant elicitor applies to a group of compounds, which triggers physiological and morphological responses within the natural defense mechanisms. Plant elicitors can help to reduce the amount of chemicals applied to crops in order to reduce infections.

CS in combination with other chemicals has been successful for the control of foliar diseases in cucumber, cantaloupe, pepper, and tomato (Abdel-Kader, El-Mougy, Aly, & Lashin, 2012). The plant defenses can be constitutive or induced and exogenous administration of different phytohormones, are reported to induce plant defenses triggering local and systemic plant responses (Tocho, Lohwasser, Börner, & Castro, 2014). In this sense, salicylic acid (SA) is a phytohormone known to play major role in several physiological processes including the regulation of plant defense response against various pathogens. SA has been well associated with resistance to biotrophic pathogens revealing that a wide range of plant defense responses is dependent on SA signaling (An & Mou, 2011).

Taking into account the low solubility of SA in water (Shalmashi & Eliassi, 2007), the development of a SA delivery system based on biocompatible polymers is a markable strategy to gain efficient control in terms of its loading and rate ofdelivery in plants. In addition, the regulation of the application doses of SA is key in the modulation of growth and defense responses of plants (http://www.mcahonduras.hn/documentos/PublicacionesEDA/Manuales%20de%20produccion). Currently, in horticulture, the development and application of more stable, sensitive and appropriate bioactives to be applied in aqueous solutions are highly valued. Lettuce is one of the most important leafy vegetables cultivated worldwide and fungal diseases are one of the main factors which affects its productivity. The abusive use of fungicides which in many cases have already show resistance to many phytopathogens (Kurzawińska, 2007; Parra et al., 2016) remains still being the commonly used strategy. In this work, we try to provide emerging tools to further develop more sustainable-based strategies for pest-management and improve growth and yield of lettuce plants.

The aim of this work was to prepared CS microparticles (MP), based on the polymer obtained from local shrimp industry waste, loading different amounts of SA in order to combine CS and SA actions triggering growth stimulation and plant defense responses with minimum impact to the environment, health and well-being.

2. Experimental

2.1. Materials

CS was synthesized in Gihon Laboratorios Químicos SRL (Mar del Plata, Argentina) from shrimp fishing industry wastes, NaOH 99% (Unipar Indupa, Argentina), glacial acetic acid 98.10% (Lotte BP Chemicals; Argentina), sodium tripolyphosphate (TPP) (Indaquim, Argentina) were used.

2.2. Synthesis of CS from local shrimp flour

CS was synthesized from exoskeleton from *Pleoticus muelleri* obtained from fish industry waste in Argentinean Patagonia through classic three step method of demineralization, deproteinization and deacetylation with modification (Puvvada, Vankayalapati, & Sukhavasi, 2012). Prior to use, CS was dissolved in 0.1 M glacial acid solution 1%(w/w) at room temperature for 2–3 h under severe stirring. Soluble CS obtained was purified by filtration to remove insoluble contaminants.

2.3. Determination of deacetylation degree (DD) by Fourier-transform infrared spectroscopy (FTIR)

The DD of independent batches of synthesized CS was determined by FTIR (Supplementary data). FTIR spectra were performed in the attenuated total reflection mode (DRS-FTIR) on a IRAffinity-1S FTIR spectrophotometer (Shimadzu, Japan). Samples were analyzed at room temperature by 16 scans, using a resolution of 4 cm^{-1}. DD was calculated according Eq. (1).

$$N-acetylation(\%) = 31.92 \times \left(\frac{A_{1318}}{A_{1380}}\right) - 12.20 \quad (1)$$

2.4. Size exclusion chromatography (SEC)

The weight-average molecular weight (M_w) and the number-average molecular weight (M_n) of CS samples were measured by SEC using a Shimadzu 20 A cromatographer (Japan), and the polydispersity was calculated from their coefficient M_w/M_n. A set of Agilent PL Aquagel-OH (30, 40 and 50) columns connected in series (300 × 7.5 mm and particle size of 8 μm) and conditioned at 28 °C was used to elute 2 mg mL^{-1} samples. Acetic acid solution (1%; pH 3.0) was used as the mobile phase at a flow of 1 mL min^{-1}. Calibration of SEC was carried out with pullulan polysaccharide standards (Polymer Laboratories, England UK) with sample injection volumes of 50 μL.

2.5. MP preparation

The CS based MP were prepared by the gelation method (Cerchiara et al., 2015) with modifications using TPP as crosslinker. Firstly, 1 L of a solution of CS (0.1 or 0.2% w/v, pH 3.0), prepared in an aqueous solution of 1% (v/v) acetic acid, was kept under vigorous stirring. When CS was completely dissolved, SA was added in different ratios (1, 5, 10 and 20% w/w with respect to CS) in order to obtain MP named as MP-1SA, MP-5SA, MP-10SA and MP-20SA, respectively, being MP-0 the unloaded MP system. After SA was totally dissolved, a TPP solution (10% w/w with respect to CS) was added dropwise (Table 1).

2.6. Obtaining of solid state MP by spray drying

Spray drying was performed in a laboratory scale Buchi Mini spray-dryer B-290 with a 1.5 mm diameter nozzle and main spray chamber of

Table 1
Physicochemical characterization: Main physicochemical properties of CS, SA and CS based MP. Size and PDI were determined by SEM analysis, and EE% was determined by UV, and thermogravimetric analysis of CS, SA and MP were determined by TGA; Peak temperatures (Tp) and final residual mass (M_r) for SA, CS and MP with different contents of SA.

Name	% SA amount (w/w respect to polymer)	Size (μm)	PDI	EE (%)	Tp(°C)	M_r800 °C (%)
CS	–	–	–	–	60.5 – 155.0 – 265.6	21.56
SA	–	–	–	–	189.9	0
MP-0	–	2.10 ± 0.78	0.14	–	53.8 –155.1 – 262.9	27.89
MP-1SA	1	1.99 ± 0.89	0.22	99	148.6–265.6	11.30
MP-5SA	5	2.45 ± 0.94	0.10	98	55.0 – 148.6 – 271.0	31.22
MP-10SA	10	2.05 ± 0.97	0.22	69	57.8 – 145.0 – 272.8	28.08
MP-20SA	20	1.57 ± 0.45	0.08	59	51.1 – 145.9 – 215.2 – 272.9	28.00

500 × 215 mm. The MP suspension was fed into the main chamber through a peristaltic pump at a feed flow rate of 8 g min^{-1}, with a drying air flow rate of 73 m^3 h^{-1} and a compressor air pressure of 0.06 MPa. Inlet and outlet temperatures were 180 °C and 100 °C, respectively.

2.7. MP characterization

2.7.1. Determination of MP size and morphology by SEM

The morphology of the spray-dried MP was evaluated by scanning electron microscopy (SEM; JEOL JSM-6100) with 15 kV. An Auto Sputter Coater 108 (Cressington, England) was used for sample coating with metallic gold for 30 s before SEM characterization to enhance the contrast of non-conducting samples. Furthermore, size distribution was also evaluated through SEM micrographs analysis. An histogram was extracted from 6 different micrographs built from 100 MP diameter measured by two different researchers using ImageJ software. The mean diameter (d) ± standard deviation (σ) value and the polydispersity index (PDI) were calculated according to Eq. (2).

$$PDI = \left(\frac{\sigma}{d}\right)^2 \quad (2)$$

2.7.2. Entrapment efficiency (EE)

The EE of SA was determined by suspending an accurately weighted amount of MP (20 mg) at a concentration of 1 mg mL^{-1} in 1% (v/v) acetic acid solution for 2 h and analyzing the amount of SA released in the resulting filtered solution (Cerchiara et al., 2015). The amount of drug was determined by UV (Shimadzu UV-1800, Japan).

The MP EE was calculated using the following Eq. (3):

$$\%EE = (\text{Total amount of SA entrapped} - \text{Amount of unbound SA}) \times 100/\text{Total amount of SA} \quad (3)$$

2.7.3. FTIR of MP

MP FTIR spectra were performed as described in Section 2.3.

2.7.4. Thermogravimetric analysis (TGA) of MP

TGA was performed in a TA Auto-MTGA Q500 Hi-Res. Three mg of free CS, TPP, MP-0, MP-1SA, MP-5SA, MP-10SA and MP-20SA samples were hermetically sealed in aluminium pans. The dynamic scans were taken in N_2 atmosphere (flow rate of 50 mL min^{-1}) in order to avoid the thermo-oxidative oxidation at the heating rate of 10 °C min^{-1}. The TGA curves were obtained in a temperature range from 25 to 800 °C.

2.7.5. Differential scanning calorimetry (DSC) of MP

DSC was carried out in a DSC Q 2000 (TA Instruments, England UK) from room temperature to 400 °C at a heating rate of 10 °C min^{-1} under N_2 atmosphere. An amount of 3 to 5 mg of each sample was used.

2.7.6. In vitro SA release

In vitro SA release from MP was investigated in water suspensions for a total period of 24 h. Briefly, 2 mL of MP suspension were incubated in tap water at 25 °C, after fixed time frame total suspensions were filtered and freezed for further quantification. SA concentration was measured by UV–vis spectrophotometry using a NanoDrop One Microvolume Spectrophotometer (Thermo Scientific, USA). The experiment was carried out in triplicate.

To estimate the mechanism of drug release, first 60% drug release data were fitted in Korsmeyer-Peppas model (Korsmeyer & Peppas, 1983) in order to better understand of the SA release mechanisms from MP.

2.8. Biological characterization

2.8.1. Plant material, growth and treatments

The butterhead lettuce (*Lactuca sativa L*, cv. Reina de Mayo) seeds were sterilized in 30% (v/v) hypochlorite and 0.2% (v/v) Tween-20 solution for 10 min, followed by 3 washing steps in sterilized distilled water. Seeds were sown under lamina flow hood on 8% (w/v) agar-H_2O in Petri plates and placed vertically in the growth chamber at 23 °C under 250 µmol photons m^{-2} s^{-1} with 16:8 h light:dark cycles. Then 3 d post-germination (dpg) seedlings were transferred to agar plates containing MP-0 or SA loaded MP, free CS and SA at indicated concentrations. Data was recorded for the length of primary root (PR) and root fresh weight (FW) after 2 and 4 d of treatment, respectively. For plant defense biochemical markers, 5 dpg seedlings were sprayed with MP-1SA, MP-0, CS or free SA, at indicated concentrations. The plant tissue was collected for immunoblotting analysis after 8 and 24 h of treatment.

2.8.2. Toxicity assessment

Inhibitory effect on the length of PR is taken as an indicator of toxicity in lettuce seddling (Lyu et al., 2018; Kummerová and Kmentová, 2004). Seedlings were photographed and PR elongation was quantified using the ImageJ image-analysis software (USA National Institutes of Health). The values shown in the figure are mean values +/− SE of 3 independent experiments (n = 36). Data is shown as relative growth respect to H_2O treatment.

2.8.3. Measurements of root fresh weights (FWs)

Root FWs of lettuce seedlings were measured with an analytical balance (Mettler model ME204, USA; sensitivity 0.1 mg). The results shown in the figure are mean values +/− SE of 3 independent experiments (n = 36).

2.8.4. Protein extraction and immunoblotting assays

Total soluble proteins were extracted from 60 mg of fresh tissue in protein extraction buffer (Agrisera, Sweden) supplemented with the protease inhibitor cocktail (Nº P9599 Sigma Aldrich, USA). After centrifugation at 12,000*g* for 15 min, supernatant was collected and boiled for 5 min in SDS-PAGE Laemmli sample buffer. Samples were run on 15% (w/v) SDS-PAGE, electrotransfered onto nitrocellulose membranes, and probed with 1:2500 NPR1 or 1:5000 PR2 primary antibodies (AS12 1854 and AS07 208, respectively, Agrisera, Sweden) overnight followed by incubation with 1:7000 anti-rabbit secondary antibody conjugated to alkaline phosphatase (Invitrogen, USA). NPR1 is a key positive regulator of the SA-dependent signaling pathway (Cao, Glazebrook, Clarke, Volko, & Dong, 1997). PR2 is a pathogenesis-related (PR) protein and is currently used as markers for innate immunity (Sudisha et al., 2012). PR2 abundance was measured at 8 h and 24 h after treatment. All immunoblotting experiments were performed in triplicate. Densitometry analysis of protein abundance was estimated using ImageJ software (USA National Institutes of Health) and expressed as arbitrary units (a.u.). Ponceau staining was used as loading control.

2.9. Statistical analysis

The data were subjected to analysis of *t*-test respect to H_2O treatment using Graphpad Prism version 5.01 software (*p < 0.05 **p < 0.01).

3. Results and discussion

3.1. CS obtained and characterized from fish industry waste

The shrimp fishing industry generates high volumes of waste from exoskeletons and heads, which has an significant environmental impact

worldwide (Yan & Chen, 2015). Particularly, in Argentina, an adequate handling of this waste allows its use for the extraction of CS, to give it a second life as potential bioactive for agriculture use. Here, the extraction of chitin and CS from the shrimp residues of *Pleoticus muelleri* was carried out in order to provide a pilot strategy to add industrial value to the local fish waste.

The coasts of the Argentinean Republic are one of the main sources of crustaceans of excellent quality in the world. The industrialization and commercialization of shrimp and prawns is an important source of resources for the country but, at the same time, it creates an enormous environmental problem: the shells of the crustaceans, discarded by the factories after the extraction of the edible part, they accumulate in huge dumpsites that constitute a serious polluting waste, representing a negative environmental impact (https://www.fishsource.org/stock_page/1473). Obtain a high quality CS from that waste, eliminating its environmental impact, and use it to the development of a microparticulated polymeric biostimulant which is biodegradable and biocompatible deals with the problem of the use of toxic pesticides to control plant diseases which impacts to the human health and environment.

The procedure to obtain chitin consists in isolating it from proteins, minerals, generally calcareous, and pigments (Rinaudo, 2006). CS, the main derivative of chitin, is obtained industrially through a deacetylation treatment. In our work, the steps of this process were deproteinization and demineralization. Depending on the reaction conditions, CS of different M_w and DD could be obtained.

Bands which corresponds to the free amino group (NH_2), mainly present in CS, could be observed between 1261 and 1029 cm^{-1}, and the peak at 1382 cm^{-1} represents the −C−O stretching of primary alcoholic group. The absorbance bands of 3268, 2930, 2850, 1562 and 1411 cm^{-1} corresponding to NH stretching, CH_3 stretching and asymmetric CH_2 stretching, CH stretching,C═O stretching in secondary amide (amide I) and C−N− stretching in secondary amide (amide II), respectively, as previously reported by Puvvada et al. (2012). To identify if there were variations in chemical functional groups present in CS samples of different molecular weight, IR spectroscopy was performed. No significant differences were seen between two CS batches instead of their different M_w (Fig. S1).

FTIR was also used to determine DD of CS obtained. Both CS analyzed in this work exhibited DD higher than 87%. DD represents a main role in the activity of CS, affecting the physico-chemical and biological properties of the polymer.

Being a natural-based polymer, it is difficult to predict CS characteristics during its production. The obtanied CS from the described process was reported to have an average M_w 1531 ± 372 kDa, M_n 559 ± 95 kDa and a polydispersity index (M_w/ M_n) of 1.95 ± 0.32 determined by SEC, which showed that the polymer was intact after the strong alkali exposure. Both CS obtained here were of very high molecular weight, since low molecular weight CS is usually characterized by M_w comprised between 20 kDa and 190 kDa. Being the main objective of the research the development of a CS based microparticulated SA delivery system with potential application as an active compound in plant CS M_w and DD plays a main role in its performance as matrix in the MP. Indeed, it was previously reported that CS with high M_w and DD present lower release profile acting as a vehicle (Ko, Park, Hwang, Park, & Lee, 2002). Since main characteristics such as solubility, biocompatibility and antimicrobial activity rises directly proportionally to high M_w and DD (Dash et al., 2011), those parameters described here fits with the main objective of this work.

3.2. MP characterization

3.2.1. MP size and morphology

CS based MP were successfully obtained through gelation method (Cerchiara et al., 2015) with modification. SEM images of the obtained CS based MP exhibited a collapsed vesicular shape (Fig. 1). This resulting morphology is associated with the electrochemical interaction between TPP and the amino free group of the deacetylated units of CS, which is protonated in an acid medium (Shu & Zhu, 2000). Also, the spray drying process causes this kind of shape in the CS-based MP. MP-0 presented a size of 2.10 µm ± 0.78 µm with PDI of 0.14, showing low polydispersity. It was previously described that electrosprayed particles morphology is directly related with droplet drying rate and the shrinkage caused by evaporation of solvents (Moreno et al., 2018). In fact, as it was previously reported when crosslinker/polymer ratio raise, MP mantain their spherical structure but had a depressed surface directly related to TPP-CS interaction. An irregular shape with a smooth surface is usual in MP as the TPP/CS mass ratio increases over 1% w/w (Desai & Park, 2005). Small amount of TPP leads to excessive degree of swelling or MP dissolution in water. Besides, MP roundness tend to decrease as TPP ratio increases due to ionic interactions between the crosslinker and CS generating crosslinked networks that modify the morphology of the particles during the drying process (Helbling et al., 2018). As it is shown in Table 1 and SEM extracted histograms (Fig. 1) all different SA loaded MP systems prepared presented a narrow size distribution with an apparent average diameter between 3.35 µm to 1.57 µm. Size and PDI of the different formulations developed were influenced by the amount of SA, showing an average size decreasing when SA amount rises (Table 1). However no statistically significant differences in size were observed between the formulations analyzed by SEM.

3.2.2. EE of MP

SA was successfully entrapped in the CS matrix with EE higher than 59% in all microparticulated systems (Table 1). The EE of the MP increased with decreasing the drug to polymer ratio, reaching the highest value when this ratio was 1–5% (w/w) of SA. SA posses a pKa of 2.78; for this reason in aqueous solution this molecule is in the anionic form which could explain the decrease in EE when the SA amount rises, due to the competitive interaction between anionic TPP and SA to bond with protonated NH_3 from CS (Bonina et al., 2007).

3.2.3. FTIR analysis confirms SA presence in the CS based MP

The CS based MP were characterized through FTIR spectroscopy (Fig. 2). The FTIR spectrum of pure sodium TPP (Fig. 2A) showed characteristic bands at 1218 cm^{-1} (PO stretching), 1156 cm^{-1} (symmetrical and asymmetric stretching vibration of the PO_2 groups), 1094 cm^{-1} (symmetric and asymmetric stretching vibration of the PO_3 groups) and 892 cm^{-1} (P−O−P asymmetric stretching). The main differences between the FTIR spectra of the particles and the raw CS, refers to a band at 892 cm^{-1} attributed to P−O−P asymmetric stretching. Moreover, the band at 1600 cm^{-1} which is attributed to NH deformation of amine groups that appears on raw CS spectrum is absent in the spectrum of MP-0 and a new band around 1550 cm^{-1}, assigned to $^{+}NH_3$, could be observed (Ji, Hao, Wu, Huang, & Xu, 2011). Therefore, from this spectral information, it could be concluded that the crosslinking was effective through ionic interactions among negatively charged PO^{-} moieties of TPP and protonated $^{+}NH_3$ moieties of CS chains.

SA loaded MP (MP-1SA, MP-5SA, MP-10SA, MP-20SA) were characterized by FTIR (Fig. 2B). Infrared spectrophotometry was chosen as a qualitative method to corroborate SA presence in CS based MP. It was possible to see evident spectral changes due to SA incorporation in different ratios when comparing the FTIR spectra of loaded and unloaded MP. SA FTIR spectrum reveals absorbance peaks at 1481 cm^{-1}, 1465 $cm^{-1}$and 1442 cm^{-1} as was previously reported (Puttipipatkhachorn, Nunthanid, Yamamoto, & Peck, 2001). Firstly, the enlargement of the two bands at 1460 cm^{-1} which is relate to C═C stretch which are attributed to the benzene ring could be observed and became more evident when SA ratio rises. Besides, enlargement in the region of 1250 cm^{-1}.On the other hand, CS absorbs IR radiation at 1660 cm^{-1} (I amide bond), 1565 cm^{-1} (II amide bond) and at

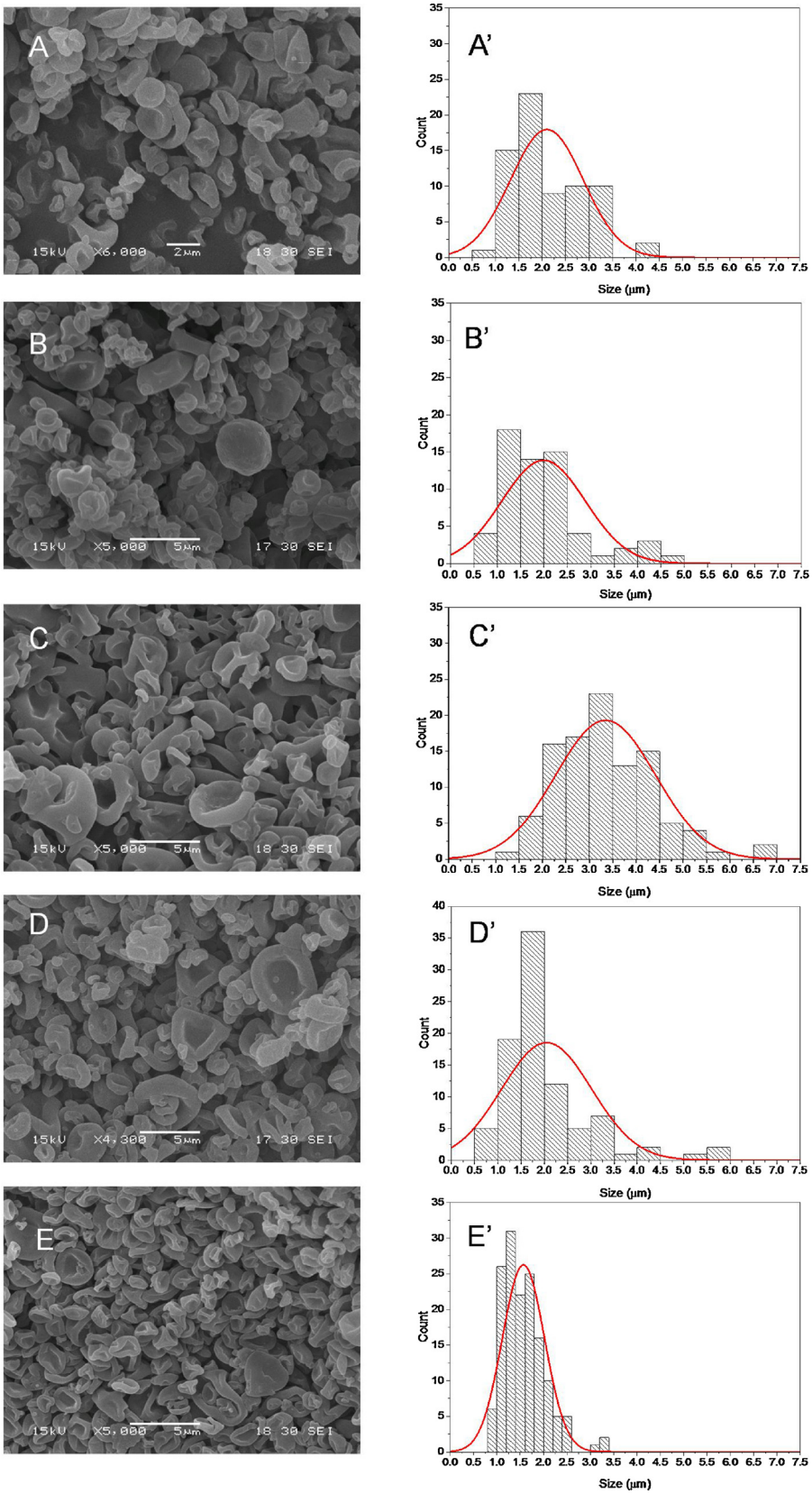

Fig. 1. Representative SEM micrographs of obtained CS based MP (A–D) and extracted histogram of MP size distribution (A'-D'). MP-0 (A and A'); MP-1SA (B and B'); MP-5SA (C and C'), MP-10SA (D and D') and MP-20SA (E and E').

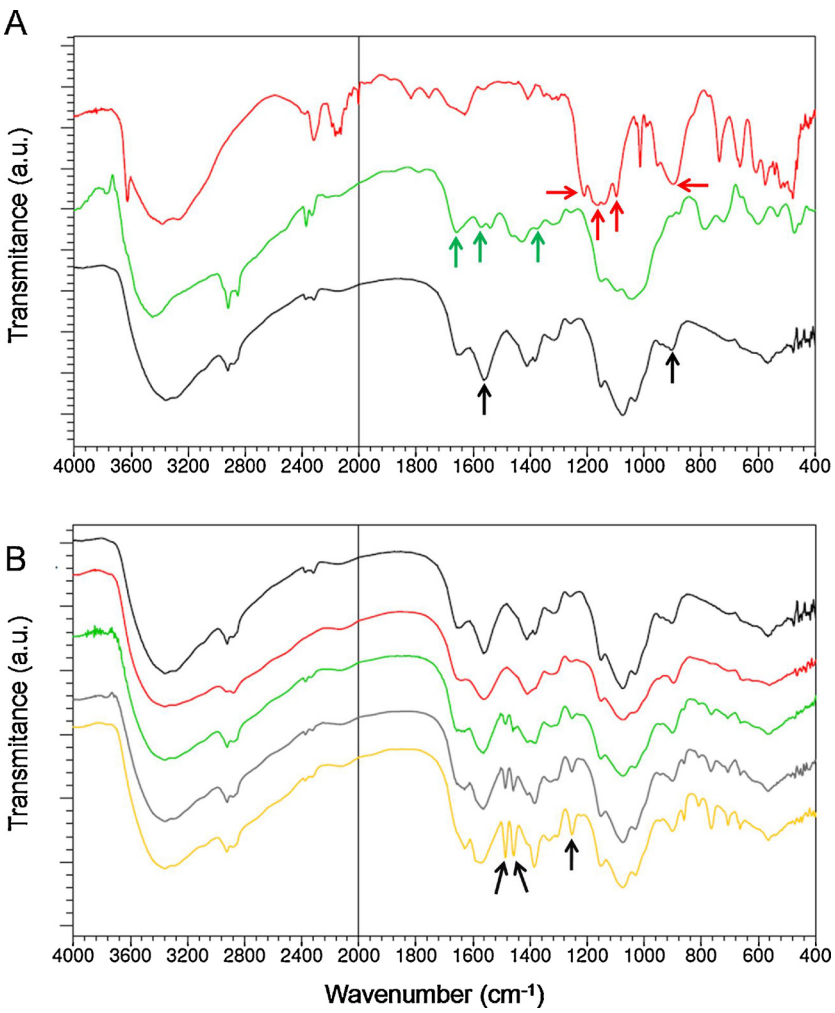

Fig. 2. Infrared spectroscopy of CS and MP. (A) FTIR spectra and relevant peaks assigned of TPP (red; 1218 cm^{-1}, PO strettching; 1156 cm^{-1}, strettching vibration of PO_2 groups; 1094 cm^{-1}, stretching vibration of PO_3 groups and 892 cm^{-1}, P—O—P asymmetric stretching), CS (green; 1660 cm^{-1}, I amide bond; 1560 cm^{-1} and 1360 cm^{-1}, II amide bond) and MP-0 (black; 1550 cm^{-1}, $^{+}NH_3$; 892 cm^{-1}, P—O—P stretching); and (B) FTIR spectra of SA loaded MP-0 (black), MP-1SA (red), MP-5SA (green), MP-10SA (grey) and MP-20SA (yellow; Black arrows indicate relevant peaks: 1480 and 1460 $cm^{-1}$and an enlargement in 1250 cm^{-1} related to the SA benzene ring) (For interpretation of the references to colour in this figure legend, the reader is referred to the web version of this article).

1360 cm^{-1} which confirms an effectiveness of SA loading by gelation technique.

At pH 3.0, CS chains were protonated with a high density of positive charges, which strongly contributes to ionic association with polyanions as TPP (Puttipipatkhachorn et al., 2001). This set of information confirms the SA entrapment due to existing electrostatic interactions among $^{+}NH_3$ and phosphate groups which supports the high efficiency in SA loading on CS/TPP MP.

3.3. Thermal analysis of SA loaded MP

Fig. 3A and B show the TGA curves obtained for SA, CS and MP with different contents of SA whereas the relevant parameters determined from these curves are summarized on Table 1.

SA displayed only one degradation peak related with its decomposition, centered around 190 °C. On the other hand, in the case of CS, 3 main peaks (centered around 54 °C, 155 °C and 263 °C) are detected. The first stages ranged between 30 and 145 °C and shows about 5% loss in weight is thought to be due to moisture vaporization. The second weight loss begins around 160 °C and the corresponding weight loss of about 60% is attributed to the decomposition of CS (Corazzari et al., 2015). The peak, which appears in the temperature range between 250 °C and 350 °C, corresponds to the decomposition ofthe polymer. Sakurai, Maegawa, and Takahashi (2000) and Zeng, Fang, and Xu (2004) also reported that the thermal degradation of CS begins at about 250 °C. Similar peaks can be also observed for MP-0 and with different contents of SA.

Fig. 3C and D show DSC curves for SA, CS and SA loaded MP. In the case of SA, a clear peak, centered at 159.8 °C, is observed. This peak can be associated to the melting point of the drug (http://www.chemicalbook.com/ChemicalProductProperty_EN_CB1680010.htm). In the case of CS, two wide peaks centered at 103.0 °C and 176.6 °C respectively, can be observed. The first peak is coincident with the dehydration of the polymer (Guinesi & Cavalheiro, 2006). Different Tg values for CS have been reported by temperature modulated DSC, *e.g.* 203 °C, 161 °C, 150 °C, and 118 °C in dry state and 61 °C in the presence of water. These observations provide evidences that water may form intermolecular hydrogen bonds and acts as plasticizer in CS. Similar behavior was displayed for unloaded and SA loaded MP. It could be observed that microvehiculization process did not affect polymer structure since raw polymer and CS-based MP exhibited the same value for relaxation enthalpy. The DSC study did not detect any crystalline drug material in the SA loaded MP whereas the endothermic peak of SA was absent. Thus, it can be concluded that SA incorporation into the MP was in an amorphous or disordered-crystalline phase of amolecular dispersion or a solid solution state in the CS matrix (Mainardes, Gremião, & Evangelista, 2006).

3.4. SA was release from MP in a sustained way

When sustained cationic active ingredient release cannot be provided by making use of a simple dissolution process, it can be achieved by using anionic polymeric excipients such as polyacrylates, sodium carboxymethylcellulose, or alginate (Prabaharan & Mano, 2004). In case of anionic molecules, CS is the only choice to a proper sustained release from a polymer matrix.

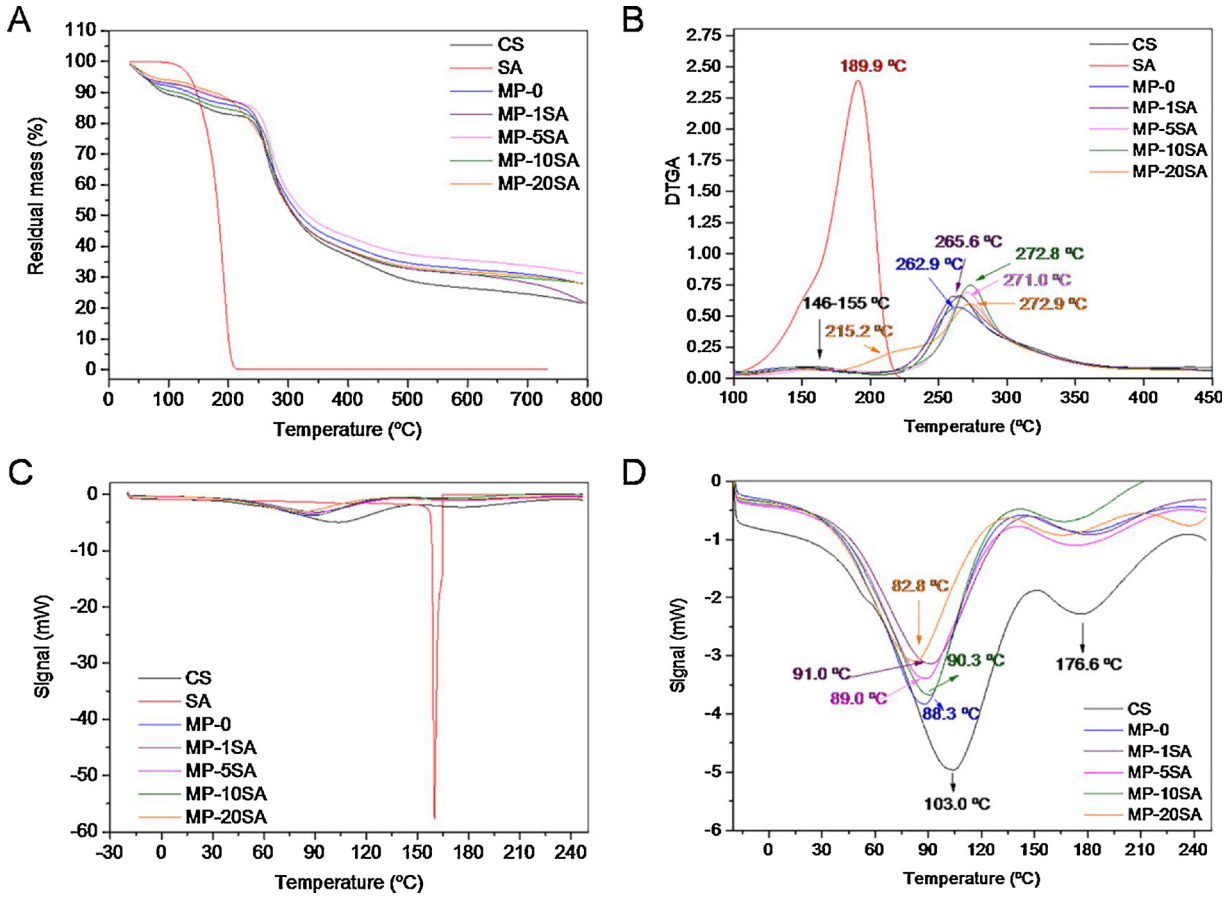

Fig. 3. MP thermal characterization. (A) Residual mass as a function of temperature (TGA curves) obtained for SA, CS and SA loaded MP. (B) Derivative of residual mass as a function of temperature (DTGA curves) obtained for SA, CS and MP with different contents of SA. (C) Heat as a function of temperature (DSC curves) for SA, CS and SA loaded MP, and (D) and amplification without SA.

The interactions between CS and SA forming the MP are based on anionic cross-linking resulting in stable complexes from which the drug can be released over a more prolonged time period. Crosslinking of biodegradable polymers is potentially important to control swelling and degradation rates. Degradable natural polymers, such as CS can be hydrolyzed in the biological milieu, in this case under the influence of water at room temperature (Prabaharan & Mano, 2004).

All the studied systems exhibited a considerable burst release effect of SA from polymeric matrix during up to the first two hours (Fig. 4A). It can be postulated that water can easily enter to the interconnected network form by polymer chains leading to hydrolytic degradation thus, releasing SA to the incubation medium. Among all the CS based MP formulations, MP-10SA and MP-1SA seem to display a more sustained release considering potential agriculture application procedures. Results shown in Fig. 4B are in accordance with the initial amount of SA loaded in each CS based microparticulated system. Emulation of the conditions that will take place when applying this SA delivery active system in plants represents a big challenge and for this reason MP biological performance plays a key role in this study.

The study of the release kinetics of a drug entrapped within a polymeric delivery system is very important because provides useful information regarding the release mechanism. In many cases the systems can be fitted using Eq. (4) proposed by Korsmeyer in 1983 and Peppas in 1985 (Korsmeyer & Peppas, 1983) which is an approximation frequently used for the modeling and analysis of drug release process in sink conditions from polymeric systems. This equation is a generalized form of the Higuchi equation and tries to explain the release mechanisms where matrix erosion or dissolution takes place.

$$\frac{M_t}{M^{\infty}} = K.\, t^n \tag{4}$$

Where M_t/M^{∞} is the fraction of the solute that has been released at a certain time t and K is a constant that includes structural and geometrical characteristics of the delivery system, and n indicates the drug release mechanism.

It is worth to notice that this n value was defined for a spherical geometry in order to characterize different release mechanisms, being a $n = 0.43$ value attributed to a Fickian diffusion, a n value between 0.43 and 0.85 to an anomalous transport and a $n = 0.85$ value to a polymer swelling controlled mechanism (Costa & Lobo, 2001). The determination of the exponent n was performed using only the data corresponding to the portion of the release curve where $M_t/M^{\infty} < 0.6$ as this model requires (Dash, Murthy, Nath, & Chowdhury, 2010).

When the release mechanism is not well known or when more than one type of the release phenomena could be involved this is a very convenient model. The n values obtained for all the studied microparticulated systems ($n_{MP\text{-}1SA} = 0.81$; $n_{MP\text{-}5SA} = 0.79$; $n_{MP\text{-}10SA} = 0.83$; $n_{MP\text{-}20SA} = 0.77$) corresponds to an anomalous transport, also known as anomalous diffusion, or drug release that is both diffusion-controlled and erosion controlled but in this case more likely refers to an overlapping of different phenomena during release, such as drug diffusion and polymer swelling (Buzzi et al., 2013; Holowka & Bhatia, 2016).

3.5. Characterization of the biological action of SA loaded MP in lettuce seedlings

The effect of new manufactured materials in lettuce seedlings where the inhibition of PR is taken as an indicator of toxicity was evaluated in

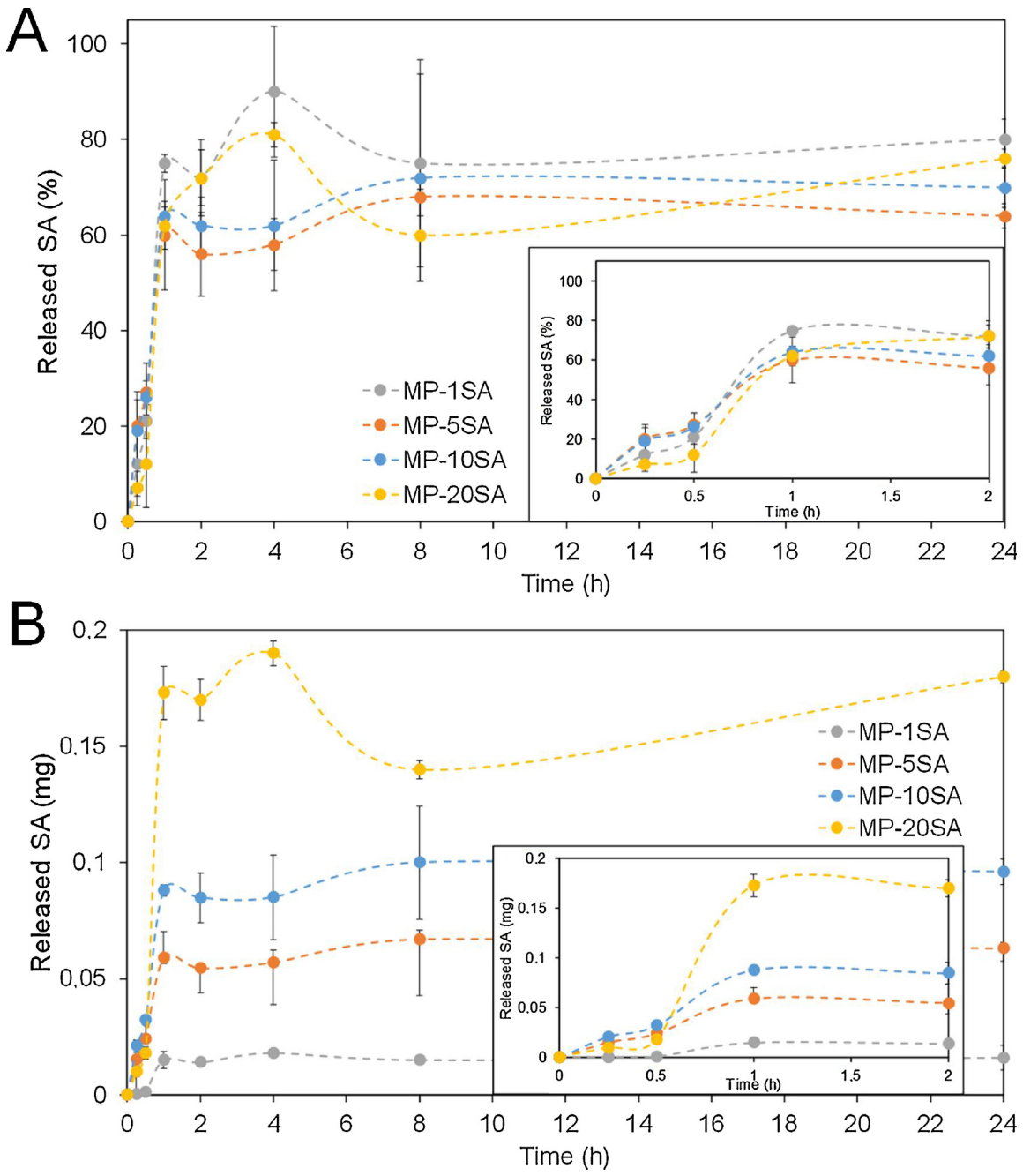

Fig. 4. 24 h *in vitro* release profile of MP-SA. (A) Data representing SA cumulative release in percentage and burst release data magnification (inner box). (B) Total amount of SA mg released and burst release data magnification (inner box). Data are mean values of 3 independent experiments ± SE.

this work (Park et al., 2016). In this bioassay 3 days post-germination (dpg) seedlings were transferred to agar plates containing medium supplemented with increasing concentrations of MP-0 or MP-SA charged with different SA doses and PR length was analysed after 2 days of treatment (Fig. 5A). The elongation of PR significantly decreased at the highest tested concentration (500 μg mL^{-1}) of all MP-SA tested. PR inhibition was also detected in seedlings treated with 50 μg mL^{-1} of MP-20SA indicating that this particles present elevated citotoxicity evidenced by a negative effect on lettuce growth. However, the elongation of PR was not reduced in seedlings treated with 0.5, 5 or 50 μg mL^{-1} of MP-1SA, MP-5SA or MP-10SA. Similar results were obtained when seedlings were treated with MP in all tested concentrations. Notably, free CS from 50 μg mL^{-1} inhibited the elongation of PR (Fig. 5A). The lower toxicity of both MP and MP-SA compared with free CS could be probably attributed to the high charge density and sensitivity of lettuce plants to the possible permeability mediated by raw CS application. Biological properties of CS are generally attributable to its cationic nature. When dissolved under acidic pH, the amino groups of the glucosamine are protonated and the cationic polyelectrolyte develops electrostatic interactions with anionic groups such as the negative lipids of cell membrane, impacting on its physicochemical equilibrium (Elgadir et al., 2015). Cell membrane permeabilization by the raw CS has been widely demonstrated in different biological systems including plant cells (Brodelius, Funk, Häner, & Villegas, 1989; Knorr & Teutonico, 1986; Young, Köhle, & Kauss, 1982). Therefore, the amount of CS applied in plants is often critical to stimulate growth processes (Lopez-Moya et al., 2017). However, when CS and TPP are mixed, the anionic TPP and policationic CS interacts leading to the formation of MP. Partially neutralized positive charges of CS allow rearrangement of chains giving emerging properties to the MP which

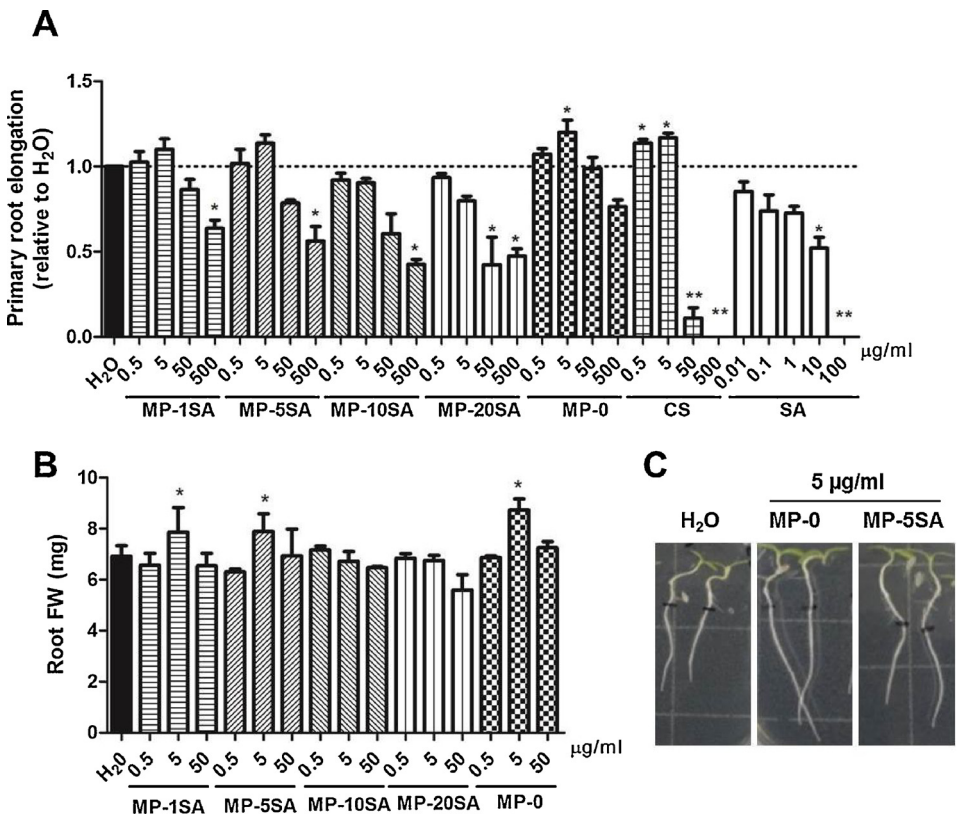

Fig. 5. Biological effect of CS based MP on lettuce root development. (A) MP-0 and MP-SA were non toxic in most of the doses applied in lettuce seedlings. Cytotoxicity assay was performed in lettuce seedlings germinated on 8% (w/v) agar-H_2O in Petri dishes. For treatments, 3 dpg seedlings were transferred to agar plates containing H_2O or increasing concentrations of MP-0 or MP-SA charged with different doses of SA as indicated. The respective controls of free CS and free SA are included. PR elongation was measured after 2 d of treatment. Relative growth respect to H_2O is shown. (B) Root FWs increase in MP and MP-SA treated seedlings.Three dpg seedlings were transferred to agar plates containing increasing concentrations of MP or MP-SA charged with different doses of SA, or H_2O as control. Root FWs were measured after 4 d of treatment. (C) Representative images from 7d old seedlings grown in 5 µg mL^{-1} MP-0 or 5 µg mL^{-1} MP-5SA or H_2O. Data are mean values of 3 independent experiments (n = 36; * $p < 0.05$ ** $p < 0.01$ T-test).

might have different accessibility to cationic groups and consequently new biological action. FTIR spectra of MP-0 which shows absency of band attributed to NH deformation of amine groups present in raw CS supports this hypothesis (Fig. 2).

In addition, seedlings treated with 5 µg mL^{-1} of MP-0 or MP-1SA or MP-5SA evidenced a slight promotion of PR elongation, revealing a positive effect of these compounds on root growth. In turn, this fact was analyzed by comparing root FWs from seedlings subjected to different treatments. Notably, a highly reproducible increament of root fresh biomass was detected in seedlings treated with 5 µg mL^{-1} of MP-0, MP-1SA and MP-5SA (Fig. 5B and C). These results indicated a dose-dependent action of each compound on the regulation of root growth in lettuce seedlings suggesting a bioactive effect on the modulation of plant physiological processes.

Since SA regulates multiple physiological responses during plant growth and development, including plant innate immunity response, the abundance of plant defense markers proteins was analyzed by immunoblotting in 5 dpg seedlings exposed to those concentrations of MP which promoted root growth.

NPR1 is described as a key regulator of the hormonal SA-dependent signaling and its content is considered an important index of pathway activation (Cao et al., 1997; Verma & Agrawal, 2017). In this work, NPR1 abundance was analyzed in 5 dpg lettuce seedlings sprayed with 5 µg mL^{-1} MP-0, MP-1SA or free CS. NPR1 was specifically and strongly up-regulated in MP-1SA treated seedlings. As expected, free SA induced NPR1 accumulation and its level was also slightly increased in CS treated seedlings when it was applied at a non-toxic concentration (Fig. 6A).

Since one of the most prominent level of the plant immune responses is the accumulation of PR proteins (Doughari, 2015), subsequently, a comparative study of the action of 5 µg mL^{-1} of MP-0 or MP-1SA on PR2 abundance was performed (Fig. 6B). Therefore, in order to trigger SA-dependent biochemical defense markers, CS was used as an elicitor instead of applying an environmental stress factor in lettuce plants. Compared with control, the application of MP-1SA and MP-0 increased the level of PR2 proteinin lettuce seedlings. Temporally differential abundance of PR2 could reveal earlier activation (at 8 h) of SA dependent pathway in MP-SA compared with MP-0 treated plants (Fig. 6B). This early effect on activation of SA dependent pathway could correlate with the burst release of drug displayed in Fig. 4. However, although PR proteins are extremely stable and resistant to proteolysis, a fine-tuning of specific metabolic reactions can be differential regulated by MP-0 or SA loaded MP and also, impact on PR2 level. In turn, we cannot discard that specific proteases probably activated upon each treatment can also differentially modulate PR2 level in lettuce plants. In fact, different signalings could be activated underlying the action of each material tested (van Loon, Rep, & Pieterse, 2006). Additionally, validated data on up regulation of PR2 protein was obtained when seedlings were placed on Petri dishes containing agar-H2O increased doses of MP-5SA (Fig. S2). However, MP-SA succesfully activated NPR1-dependent SA plant defense response. In summary, the application of MP-SA constitute highly promising bioactives to be used as new biocompatible materials, stable and with beneficial biological properties including the enhancement of lettuce plant growth and activation of the SA-dependent plant defense response required for a proper protection against biotic stress.

4. Conclusions

All MP tested had a dose-dependent toxicity and were toxic only at the highest assayed doses.The lower toxicity of MP compared with free CS was probably attributed to the microstructure obtained with gelation method which allows to a better interaction with plant with a major surface of contact, and reduce the number of exposed $^{+}NH_3$ groups that could altered cell membrane potential. MP had a positive effect in a wide range of doses on lettuce growth and induced PR2 defense marker proteins. SA loaded MP had a surpassing effect since they clearly activates NPR1-dependent SA signaling and also an earlier trigger PR2 protein abundance and activated the SA-dependent defense response in lettuce seedlings. The present study shows that the

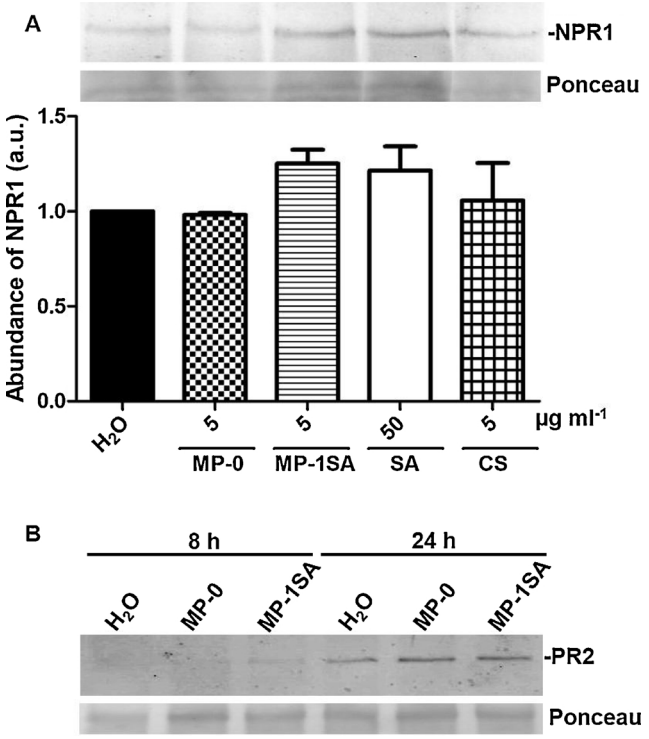

Fig. 6. The abundance of NPR1 and PR2 proteins increased in MP-1SA treated seedlings. Five dpg seedlings were treated with 5 μg mL^{-1} MP-0 or MP-1SA and H_2O, SA or CS as controls. (A) Top: Immunoblotting showing relative levels of NPR1 protein isolated from 24 h treated leaves as indicated. Bottom: Histogram expressing protein abundance related to the reference of an unknown-protein detected by Ponceau staining for each indicated treatment. Protein abundance was calculated by densitometry analysis using ImageJ software and expressed as a.u. Data are mean values of 3 independent experiments ± SE. (B) Immunoblotting showing a time-course analysis of PR2 isolated from 8 h and 24 h treated leaves as indicated (upper panel). Equivalent loading of each sample is indicated by Ponceau staining of Rubisco protein (lower panel).

application of MP and SA loaded MP is very promising as activators of SA dependent plant defense responses in lettuce seedlings, dealing with the need of new eco-friendly fertilizers. MP application as an elicitor in other crop species is promissory and merit further investigation.

Acknowledgments

Authors would liketo thank to Melina Bracone and Andrés Torres for their technical help and supported in DSC and TGA analysis. Authors would like to thank specially to Dr. Raquel Palao Suay for her help in SEC analysis. This research was partially supported by ANPCyT, CONICET and UNMDP and Gihon Laboratorios Químicos SRL. M.J.I and C.A.C are researchers from CONICET. S.L.C is a fellow from the same institution.

Appendix A. Supplementary data

Supplementary material related to this article can be found, in the online version, at doi:https://doi.org/10.1016/j.carbpol.2018.08.019.

References

Abdel-Kader, M., El-Mougy, N. S., Aly, M., & Lashin, S. (2012). Integration of biological and fungicidal alternatives for controlling foliar diseases of vegetables under greenhouse conditions. *International Journal of Agriculture and Forestry, 2*(2), 38–48.

An, C., & Mou, Z. (2011). Salicylic acid and its function in plant immunity. *Journal of Integrative Plant Biology, 53*(6), 412–428.

Atay, E., Fabra, M. J., Martínez-Sanz, M., Gomez-Mascaraque, L. G., Altan, A., & Lopez-Rubio, A. (2017). Development and characterization of chitosan/gelatin electrosprayed microparticles as food grade delivery vehicles for anthocyanin extracts. *Food Hydrocolloids, 77*, 699–710.

Bellich, B., D'Agostino, I., Semeraro, S., Gamini, A., & Cesàro, A. (2016). "The good, the bad and the ugly" of chitosans. *Marine Drugs, 14*(5), 99.

Bonina, F., Giannossi, M., Medici, L., Puglia, C., Summa, V., & Tateo, F. (2007). Adsorption of salicylic acid on bentonite and kaolin and release experiments. *Applied Clay Science, 36*(1–3), 77–85.

Brodelius, P., Funk, C., Häner, A., & Villegas, M. (1989). A procedure for the determination of optimal chitosan concentrations for elicitation of cultured plant cells. *Phytochemistry, 28*(10), 2651–2654.

Buzzi, V., Brudner, M., Wagner, T. M., Bazzo, G. C., Pezzin, A. P. T., & Silva, D. A. K. (2013). Caboxymetylcellulose/gelatin blends loaded with piroxicam: Preparation, characterization and evaluation of in vitro release profile. *Journal of Encapsulation and Adsorption Sciences, 3*(04), 99.

Cao, H., Glazebrook, J., Clarke, J. D., Volko, S., & Dong, X. (1997). The Arabidopsis NPR1 gene that controls systemic acquired resistance encodes a novel protein containing ankyrin repeats. *Cell, 88*(1), 57–63.

Cerchiara, T., Abruzzo, A., Di Cagno, M., Bigucci, F., Bauer-Brandl, A., Parolin, C., ... Luppi, B. (2015). Chitosan based micro-and nanoparticles for colon-targeted delivery of vancomycin prepared by alternative processing methods. *European Journal of Pharmaceutics and Biopharmaceutics, 92*, 112–119.

Corazzari, I., Nisticò, R., Turci, F., Faga, M. G., Franzoso, F., Tabasso, S., ... Magnacca, G. (2015). Advanced physico-chemical characterization of chitosan by means of TGA coupled on-line with FTIR and GCMS: Thermal degradation and water adsorption capacity. *Polymer Degradation and Stability, 112*, 1–9.

Costa, P., & Lobo, J. M. S. (2001). Modeling and comparison of dissolution profiles. *European Journal of Pharmaceutical Sciences, 13*(2), 123–133.

Dash, M., Chiellini, F., Ottenbrite, R., & Chiellini, E. (2011). Chitosan—A versatile semi-synthetic polymer in biomedical applications. *Progress in Polymer Science, 36*(8), 981–1014.

Dash, S., Murthy, P. N., Nath, L., & Chowdhury, P. (2010). Kinetic modeling on drug release from controlled drug delivery systems. *Acta Poloniae Pharmaceutica, 67*(3), 217–223.

Desai, K., & Park, H. (2005). Preparation of cross-linked chitosan microspheres by spray drying: Effect of cross-linking agent on the properties of spray dried microspheres. *Journal of Microencapsulation, 22*(4), 377–395.

Doughari, J. (2015). An overview of plant immunity. *Journal of Plant Pathology & Microbiology, 6*(11) 10.4172.

El Hadrami, A., Adam, L. R., El Hadrami, I., & Daayf, F. (2010). Chitosan in plant protection. *Marine Drugs, 8*(4), 968–987.

Elgadir, M. A., Uddin, M. S., Ferdosh, S., Adam, A., Chowdhury, A. J. K., & Sarker, M. Z. I. (2015). Impact of chitosan composites and chitosan nanoparticle composites on various drug delivery systems: A review. *Journal of Food and Drug Analysis, 23*(4), 619–629.

Guinesi, L. S., & Cavalheiro, E. T. G. (2006). The use of DSC curves to determine the acetylation degree of chitin/chitosan samples. *Thermochimica Acta, 444*(2), 128–133.

Helbling, I. M., Busatto, C. A., Fioramonti, S. A., Pesoa, J. I., Santiago, L., Estenoz, D. A., & Luna, J. A. (2018). Preparation of TPP-crosslinked chitosan microparticles by spray drying for the controlled delivery of progesterone intended for estrus synchronization in cattle. *Pharmaceutical Research, 35*(3), 66.

Holowka, E., & Bhatia, S. K. (2016). *Drug delivery*. Springer.

Ji, J., Hao, S., Wu, D., Huang, R., & Xu, Y. (2011). Preparation, characterization and in vitro release of chitosan nanoparticles loaded with gentamicin and salicylic acid. *Carbohydrate Polymers, 85*(4), 803–808.

Kanmani, P., Jeyaseelan, A., Kamaraj, M., Sureshbabu, P., & Sivashanmugam, K. (2017). Environmental applications of chitosan and cellulosic biopolymers: A comprehensive outlook. *Bioresource Technology, 242*, 295–303.

Knorr, D., & Teutonico, R. (1986). Chitosan immobilization and permeabilization of Amaranthus tricolor cells. *Journal of Agricultural and Food Chemistry, 34*(1), 96–97.

Ko, J., Park, H., Hwang, S., Park, J., & Lee, J. (2002). Preparation and characterization of chitosan microparticles intended for controlled drug delivery. *International Journal of Pharmaceutics, 249*(1–2), 165–174.

Kong, M., Chen, X. G., Xing, K., & Park, H. J. (2010). Antimicrobial properties of chitosan and mode of action: A state of the art review. *International Journal of Food Microbiology, 144*(1), 51–63.

Korsmeyer, R., & Peppas, N. (1983). *Swelling-controlled delivery systems for pharmaceutical applications: Macromolecular and modelling considerations.* New York: Marcel Dekker.

Kummerová, M., & Kmentová, E. (2004). Photoinduced toxicity of fluoranthene on germination and early development of plant seedling. *Chemosphere, 56*(4), 387–393.

Kurzawińska, H. (2007). Potential use of chitosan in the control of lettuce pathogens. *Polish Chitin Society, Monograph, 12*, 173–178.

Lopez-Moya, F., Escudero, N., Zavala-Gonzalez, E. A., Esteve-Bruna, D., Blázquez, M. A., Alabadí, D., ... Lopez-Llorca, L. V. (2017). Induction of auxin biosynthesis and WOX5 repression mediate changes in root development in Arabidopsis exposed to chitosan. *Scientific Reports, 7*(1), 16813.

Lyu, J., Park, J., Pandey, L. K., Choi, S., Lee, H., De Saeger, J., ... Han, T. (2018). Testing the toxicity of metals, phenol, effluents, and receiving waters by root elongation in *Lactuca sativa* L. *Ecotoxicology and Environmental Safety, 149*, 225–232.

Mainardes, R. M., Gremião, M. P. D., & Evangelista, R. C. (2006). Thermoanalytical study of praziquantel-loaded PLGA nanoparticles. *Revista Brasileira de Ciências Farmacêuticas, 42*(4), 523–530.

Mishra, S., Keswani, C., Abhilash, P., Fraceto, L. F., & Singh, H. B. (2017). Integrated approach of agri-nanotechnology: Challenges and future trends. *Frontiers in Plant Science, 8*.

Moreno, J. A. S., Mendes, A. C., Stephansen, K., Engwer, C., Goycoolea, F. M., Boisen, A., ... Chronakis, I. S. (2018). Development of electrosprayed mucoadhesive chitosan

microparticles. *Carbohydrate Polymers, 190*, 240–247.
Park, J., Yoon, J.-h., Depuydt, S., Oh, J.-W., Jo, Y.-m., Kim, K., ... Han, T. (2016). The sensitivity of an hydroponic lettuce root elongation bioassay to metals, phenol and wastewaters. *Ecotoxicology and Environmental Safety, 126*, 147–153.
Parra, L., Maisonneuve, B., Lebeda, A., Schut, J., Christopoulou, M., Jeuken, M., & Michelmore, R. (2016). Rationalization of genes for resistance to Bremia lactucae in lettuce. *Euphytica, 210*(3), 309–326.
Prabaharan, M., & Mano, J. (2004). Chitosan-based particles as controlled drug delivery systems. *Drug Delivery, 12*(1), 41–57.
Prashanth, K. H., & Tharanathan, R. (2007). Chitin/chitosan: Modifications and their unlimited application potential—An overview. *Trends in Food Science & Technology, 18*(3), 117–131.
Puttipipatkhachorn, S., Nunthanid, J., Yamamoto, K., & Peck, G. (2001). Drug physical state and drug–polymer interaction on drug release from chitosan matrix films. *Journal of Controlled Release, 75*(1), 143–153.
Puvvada, Y. S., Vankayalapati, S., & Sukhavasi, S. (2012). *Extraction of chitin from chitosan from exoskeleton of shrimp for application in the pharmaceutical industry*.
Rinaudo, M. (2006). Chitin and chitosan: Properties and applications. *Progress in Polymer Science, 31*(7), 603–632.
Ryan, C. A. (1987). Oligosaccharide signalling in plants. *Annual Review of Cell Biology, 3*(1), 295–317.
Sakurai, K., Maegawa, T., & Takahashi, T. (2000). Glass transition temperature of chitosan and miscibility of chitosan/poly (N-vinyl pyrrolidone) blends. *Polymer, 41*(19), 7051–7056.
Shalmashi, A., & Eliassi, A. (2007). Solubility of salicylic acid in water, ethanol, carbon tetrachloride, ethyl acetate, and xylene. *Journal of Chemical and Engineering Data, 53*(1), 199–200.
Shu, X., & Zhu, K. (2000). A novel approach to prepare tripolyphosphate/chitosan complex beads for controlled release drug delivery. *International Journal of Pharmaceutics, 201*(1), 51–58.
Sudisha, J., Sharathchandra, R., Amruthesh, K., Kumar, A., & Shetty, H. S. (2012). *Pathogenesis related proteins in plant defense response. Plant defence: biological control*. Springer379–403.
Tharanathan, R. N., & Kittur, F. S. (2003). *Chitin—The undisputed biomolecule of great potential*.
Tocho, E., Lohwasser, U., Börner, A., & Castro, A. (2014). Mapping and candidate gene identification of loci induced by phytohormones in barley (Hordeum vulgare L.). *Euphytica, 195*(3), 397–407.
van Loon, L. C., Rep, M., & Pieterse, C. M. (2006). Significance of inducible defense-related proteins in infected plants. *Annual Review of Phytopathology, 44*, 135–162.
Verma, K., & Agrawal, S. (2017). *Salicylic acid-mediated defence signalling in respect to its perception, alteration and transduction. Salicylic acid: A multifaceted hormone*. Springer97–122.
Yan, N., & Chen, X. (2015). Don't waste seafood waste: Turning cast-off shells into nitrogen-rich chemicals would benefit economies and the environment. *Nature, 524*(7564), 155–158.
Yang, J., Lu, H., Li, M., Liu, J., Zhang, S., Xiong, L., ... Sun, Q. (2017). Development of chitosan-sodium phytate nanoparticles as a potent antibacterial agent. *Carbohydrate Polymers, 178*, 311–321.
Young, D. H., Köhle, H., & Kauss, H. (1982). Effect of chitosan on membrane permeability of suspension-cultured Glycine max and Phaseolus vulgaris cells. *Plant Physiology, 70*(5), 1449–1454.
Zeng, M., Fang, Z., & Xu, C. (2004). Effect of compatibility on the structure of the microporous membrane prepared by selective dissolution of chitosan/synthetic polymer blend membrane. *Journal of Membrane Science, 230*(1), 175–181.